PHYSICS 4AL

EXPERIMENT 6 & 7: HARMONIC OSCILLATOR: PHYSICAL PENDULUM AND WAVES ON A VIBRATING STRING

Terrence Ho | ID: 804793446
Date of Lab: May 23th and 30th, 2017
Lab Section: Tuesday, 5 P.M.
T.A.: David Bauer
Lab Partners: Robathan Harries
Abstract: 165 words
Report: 2189 words

Contents

Abstract 2
Introduction 3
Methods 3
    Part I 3
    Part II 4
Analysis 5
    Part I: Harmonic Oscillations of a Physical Pendulum 5
    Part II: Oscillations of a Vibrating String 10
Conclusion 13
References 14

INVESTIGATING HARMONIC MOTION OF A PHYSICAL PENDULUM AND THE WAVES OF A VIBRATING SPRING

T. Ho[1]

In mechanical physics, harmonic motion is the oscillatory motion of an object where the restoring force increases with displacement and opposite the direction of motion. Harmonic motion can occur with a physical pendulum if it is displaced from its equilibrium position. Harmonic motion also occurs in non-rigid objects, such as a string, where each particle of the string is vibrated and oscillates back and forth. We sought to study these two forms of harmonic motion in our experiment. Specifically we studied frequencies of damped and driven oscillations for physical pendulums, to gain an understanding of how oscillations are controlled and created. We found the resonant frequency was 0.714 ± 0.005 Hz. In the second part of our experiment, we measured the wave speed travelling along a vibrating spring, and investigated the effects of adding a boundary condition to the middle of the string. The wave speed calculated in our experiment was ± m/s.

[1]Henry Samueli School of Engineering and Applied Science, University of California, Los Angeles

INTRODUCTION

Sidney Colman once said: "The career of a young theoretical consists of treating the harmonic oscillator in ever-increasing levels of abstraction." However, even at a level with no abstractions, we examples of harmonic oscillations in many systems of motion; we studied two of these systems in this experiment, one involving a physical pendulum and the other vibrating strings. Although these two motions may seem physically very different, a model of harmonic motions can be found in both physical systems.

With the pendulum, we examined two areas of harmonic motion: damping and driven harmonic motion. Damping occurs when an external force results in a decrease in amplitude over time. There are three damping regimes, underdamped, overdamped, and critically damped. We also studied driven harmonic motion with our swinging pendulum. The driving frequency occurs when the oscillatory motion produced by a constant outside force is at its greatest.

Vibrating strings are also a interesting because the vertical motion induced on a string creates an oscillatory motion similiar to that of a physical pendulum. Each particle on a string oscillates in relation to particles near it. Furthermore, if the string is vibrated at certain frequencies, the string produces standing waves, with the number of waves varying with the frequency at which the wave is vibrated at. We investigate these properties of vibrating strings in our experiment. (More?)

METHODS

Part I

In the first part of our experiment, we setup our equipment in the fashion shown in **Figure 6.1**. (We used a photogate to determine a start position from which to release the pendulum from.) We attached a wave driver and rotation sensor to our recording equipment, and set a high sampling rate to record data at, perhaps 50 Hz (If it is too low, the maxima in wave patterns can't be detected). We did six trials with the pendulum, one without the damping magnets and 5 with. For each trial, we recorded the time and angle of the pendulum as it oscillated. We also wanted to dertemine critical damping, so we looked at our five previous damped trials to approximate where the critical damping spot was and adjusted the magnet spacing until we achieved critical damping

Next, we began the harmonic motion with driving part of the experiment. We set the magnet spacing so that the magnets will damp out the free undriven osciallltions in about 5 to 10 seconds, (in our case 30 mm). We first want to find the damped, driven resonant frequency ω_r. Record three Lissajous figures whose x-axis are Output Voltage (V) and y-axis is angle(rad), one at the resonant frequency, one below the resonant frequency, and one above. We determined the driven resonant frequency by looking for the Lissajous plot that was symmetric.

Lastly, using the drive frequency we found in the last part, we recorded frequency and amplitudes of ten different drive frequencies. When plotted, this data should appear similar to a resonant curve,

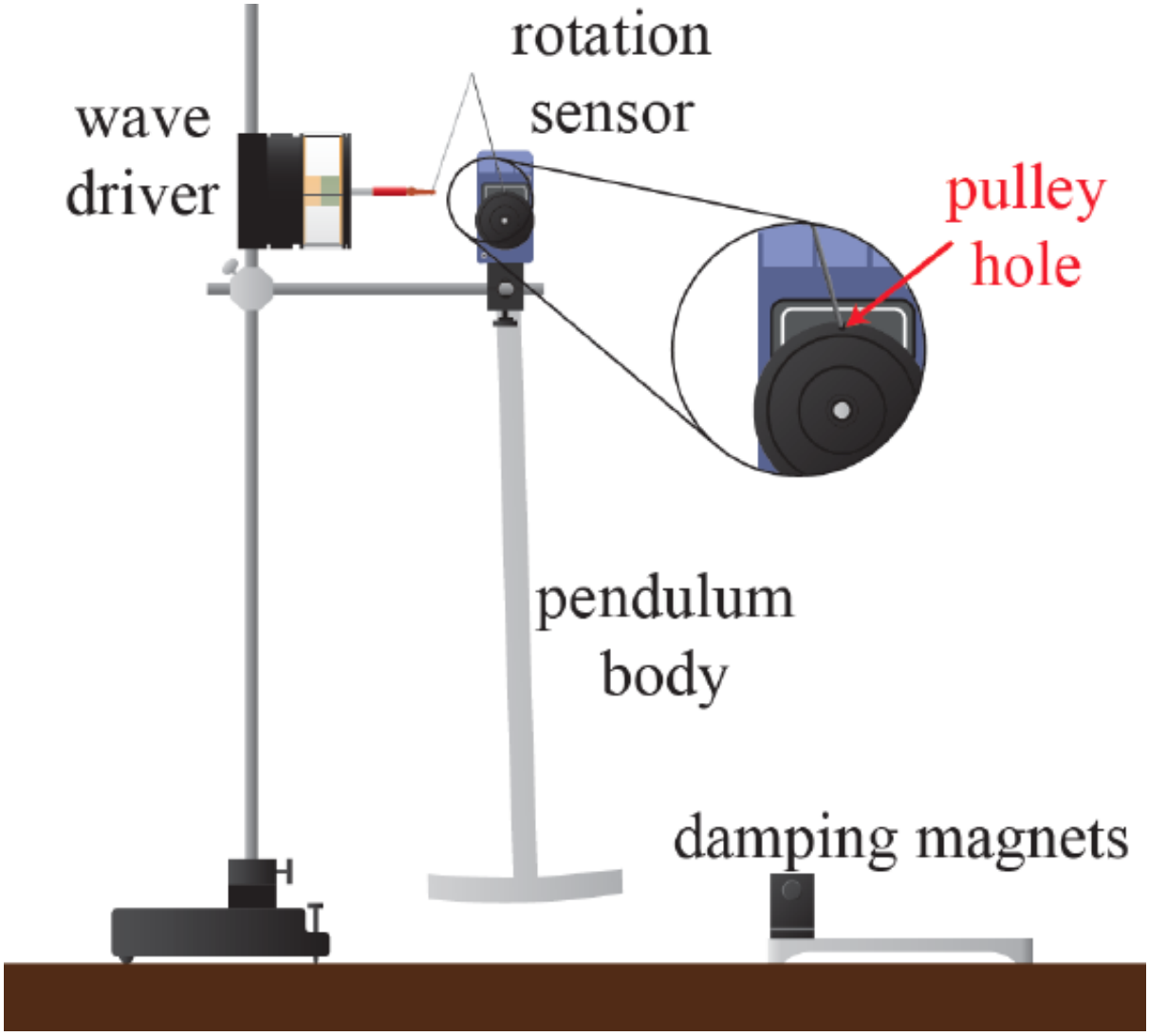

Figure 6.1 Set up for Part I of Physical Pendulum Figure reproduced (with permission) from Fig 6.1 by Campbell, W. C. et al.[1]

with the drive frequency as the peak.

Part II

In Part II of our experiment we studied waves of a vibrating spring. Our experiment setup is shown in **Figure 6.2**. We first wanted to measure the wave speed for several values of tension by varying the mass hung over the wheel. However, because linear mass density changes with different stretching, we had to recalculate linear mass density for each trial by dividing the mass of the string by the new length. We took three trials of wave speed, with at least one mass greater than 350 g (which will be used in later parts of the experiment). We configured our signal generator according to **Figure 6.3**. We set a high recording frequency to ensure the data generated included the peaks of the oscillations, and

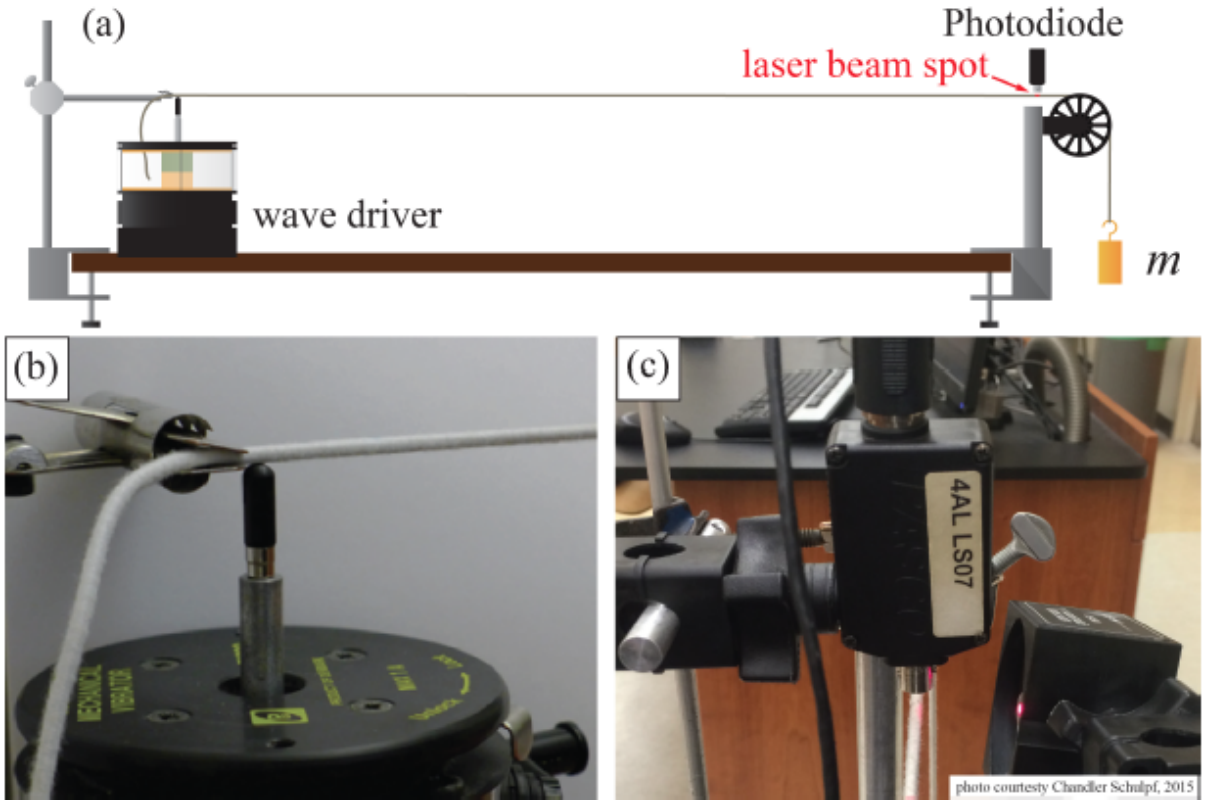

Figure 6.2 Set up for Part II of Experiment Equipment shown above used to study waves on a vibrating string. (a) and (b) depict a driver that produces vibrations on the string. The vibrations are monitored by a photodetector that shines a laser beam onto the string in (c). Figure reproduced (with permission) from Fig. 7.1 by Campbell, W. C. et al.[1]

recorded data of time (s), Light Intensity (%), and Output Voltage Ch01 (V).

Next, we wanted to study standing waves on a vibrating string. Using the weight greater than 350 g, we experimented with the driving frequency until we found the fundamental mode of resonance. We plotted Lissajous figures once again to find the fundamental mode. We found the other nodes of resonance up to the tenth node by adjusting the frequency around the nth multiple of the fundamental node.

Lastly, the string was driven at resonant frequencies for n = 2, 4, and 5 twice, once with a clamp in the middle of the string and once without. We recorded the amplitudes for three frequencies.

ANALYSIS

Part I: Harmonic Oscillations of a Physical Pendulum

In our first part of the experiment, we looked at undriven harmonic motion of pendulums. There are three regimes of oscillation, which were previously mentioned.

Figure 6.3 Caption Settings for Signal Generator Using the Signal Generator to measure wave speed. Figure reproduced (with permission) from Fig. 7.2 by Campbell, W. C. et al.[1]

1. Underdamped motion: $\omega_0 > \frac{1}{\tau}$.
2. Overdamped motion: $\omega_0 < \frac{1}{\tau}$.
3. Critically damped motion: $\omega_0 = \frac{1}{\tau}$.

Damping time τ is the time it takes for an oscillation to decay exponentially by a factor of $\frac{1}{e}$. These three regimes of oscillatory motion are shown in **Figure 6.4**. To obtain these figures, we recorded one trial on oscillation with no damping magnets, then 5 trials of successively higher damping (with magnet spacing of 50 mm, 40 mm, 30 mm, 20 mm, 10mm). Critical damping was achieved with a magnet spacing of 15.0 ± 0.5 mm. If the gap between magnets were less, we started to experience overdamped motion.

We can see that undamped motion of the pendulum in **Figure 6.4** became experienced oscillations whose amplitudes decreased slightly over time. On the other hand, critically damped and overdamped oscillations reached the equilibrium point and did not move past this point, coming to rest. We can see that the crticially damped oscillation reached the equilibrium point the fastest, which is what we expect. We determined the ω_0 by zooming in to the underdamped graph and looking at when the maxima of the oscillations appeared. $\omega_0 = 0.714 \pm 0.005$ rads/sec.

In the next section of our experiment, we looked into driven oscillations. For the following driven damped analysis, we used a damping gap of 30 mm. We assumed the damped driven oscillation

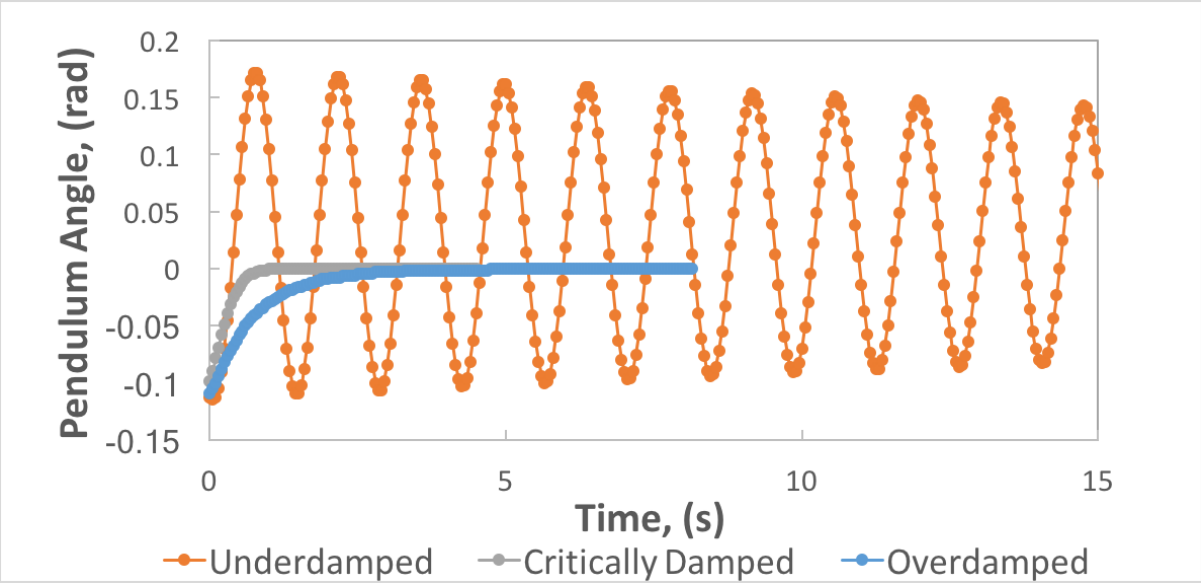

Figure 6.4 Pendulum angle against time for underdamped, overdamped, and critically damped motion. The critically damped oscillation (with a magnet spacing of 15.0 ± 0.5 mm) reached the equilibrium point the fastest compared to the other types of motion. The data points were joined by lines to make sure the different types of damping were clear.

resonance ω_R is equal to the previously found ω_0, because the damping is low. To confirm that $\omega_R \approx \omega_0$, we plottedj Lissajous plots of angle and output voltage. We will know that we will have found ω_R when the Lissajous plot is symmetric on both sides. In **Figure 6.5**, we plotted three Lissajous figures, with **(a)** being below resonance(due to left tilt), **(b)** being above resonance (due to right tilt), and **(c)** being at resonance.

By looking at these Lissajous plots, we can determine that ω_R is indeed 0.714 ± 0.005 Hz (the uncertainty was derived by looking at the tilts of the plots above and below resonance, and determining the difference).

We can also determine the damping time of the physical pendulum by looking at the peaks of **Figure 6.6** and calculating the ratios of successive amplitudes of the peaks, using the formula

$$\tau = -\frac{T}{\ln(\frac{F(t+T)}{F(t)})}$$

We calculate that the mean damping time to be 1.86 ± 0.04 s.

Now that we have the resonant frequency ω_R and the damping time, we can find th Q-factor of the physical pendulum, using the equation

$$Q \equiv \frac{1}{2}\tau\omega_R$$

We find that the Q-factor of the system is 0.66 ± 0.08 (uncertainty found by propagation of uncertainties).

There is also another way to find the Q-factor of the system, but finding the amplitudes of the

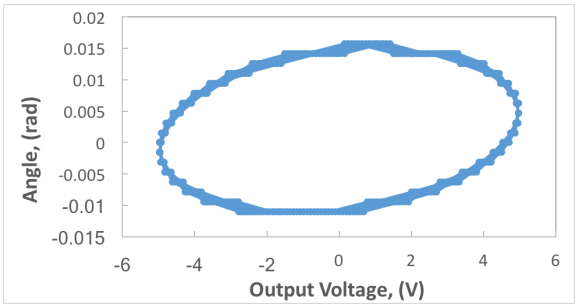

(a)

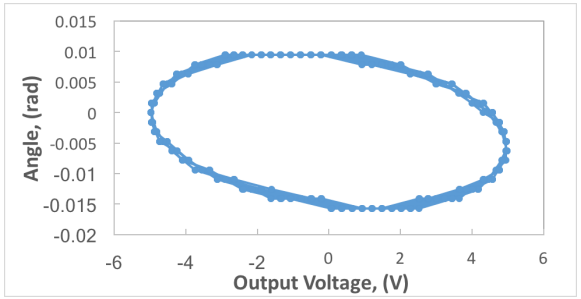

(b)

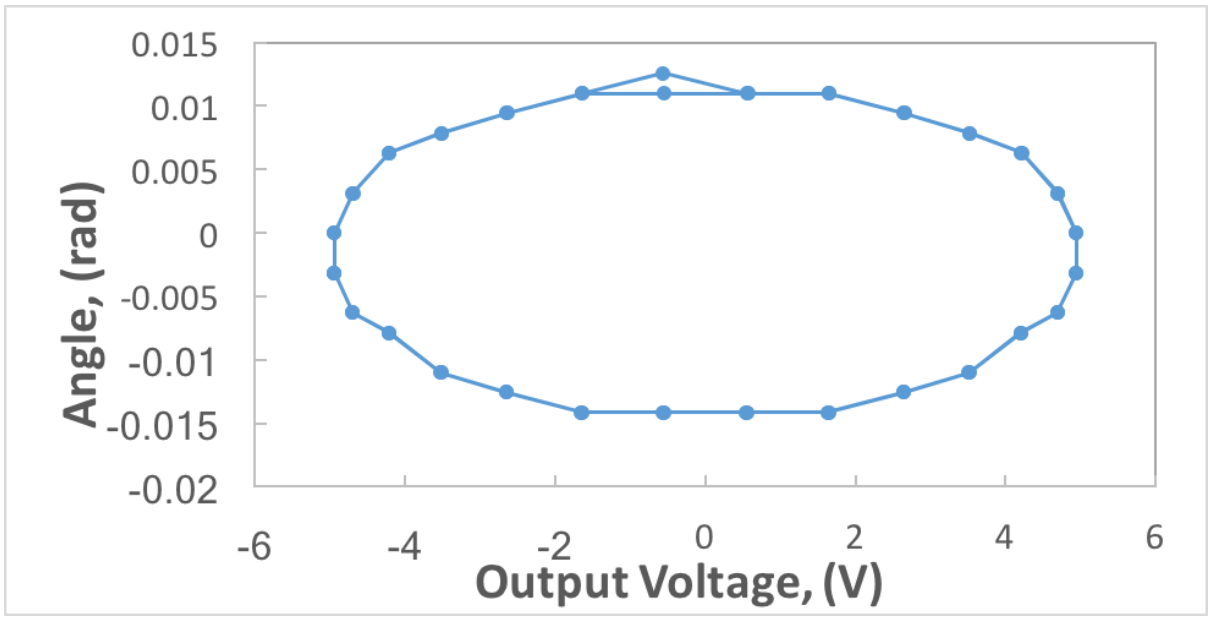

(c)

Figure 6.5 Lissajous plots below, above, and at resonance. Parametric plots of Angle (rad) vs Output voltage (V). (a) shows drive frequency below resonance, (b) shows drive frequency above resonance, and (c) shows drive frequency at resonance. The data points are joined to make the Lissajous Figures more apparent.

oscillation at frequencies around the drive frequency ω_R, known as the amplitude response. We plotted 10 frequencies in total, some above and below the resonant driving frequency, in **Figure 6.7**. We can define Q as the ratio of resonant frequency and the width of the resonant curve, or

$$Q \approx \frac{\omega_0}{\Delta\omega}$$

$\Delta\omega$ is equal to $\frac{1}{\sqrt{2}}$ of the maximum amplitude, which in this case is 0.013 ± 0.009. $\Delta\omega = 0.19 \pm 0.05$. We can find that the Q-factor = 3.76 ± 0.06 (uncertainties found by propagation of uncertainties).

The two values of Q that are completely outside their uncertainty boundaries. This can be caused by the large uncertainty in finding the $\Delta\omega$. Also, the amplitude response method of finding the Q-factor is very sensitive to exact frequencies since the amplitude is a function of frequency. If frequency values have a large uncertainty, then the Q-factor could end up with a large uncertainty and wrong value.

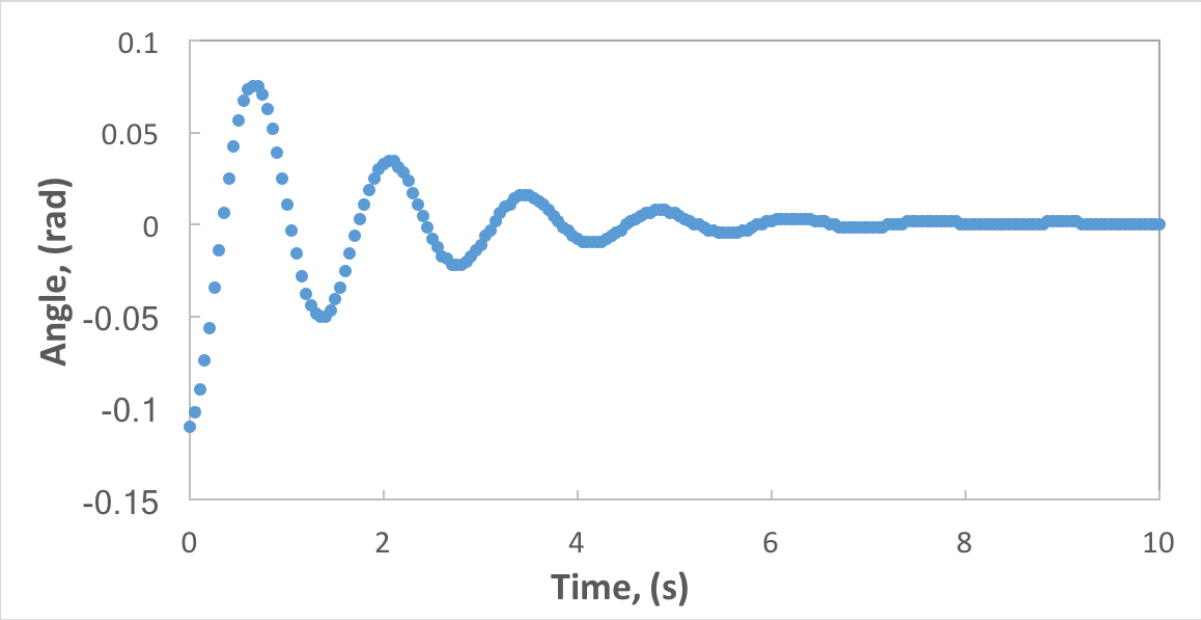

Figure 6.6 Undriven Damped Oscillations of Pendulum The damping space used for this oscillation was 30 mm.

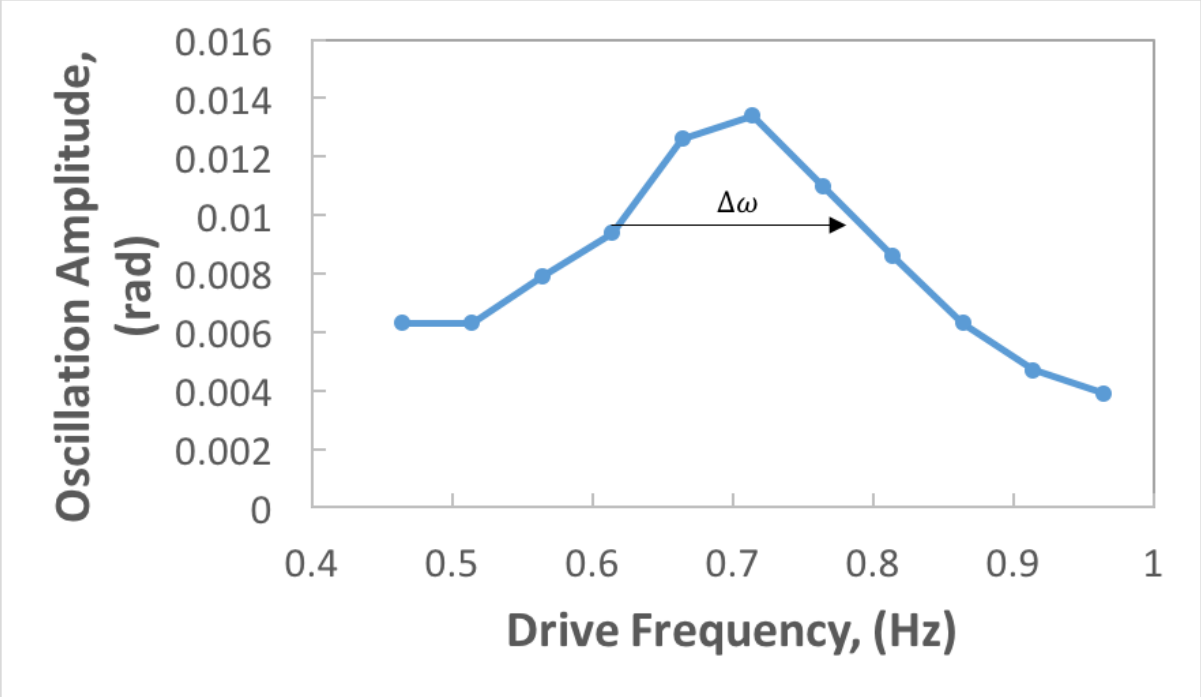

Figure 6.7 Amplitude Response of Oscillations around Drive Frequency The points indicate the oscillation amplitude in radians for the driving frequency. By joining the points, we form a Lorentzian shape. The resonance width is 1.9 ± 0.5 Hz.

Part II: Oscillations of a Vibrating String

As stated before, the individual particles of a vibrating string mimic harmonic motion by oscillating up and down. This oscillations forms waves that travel along the string. In the first part of our experiment we tried to predict the velocities of these waves as they travel along the string.

For a string that has tension T and linear mass density μ, the wave velocity is given by $v = \sqrt{\frac{T}{\mu}}$. However, because μ changes as it is stretched as a function of the length, we need to recalculate μ for different amounts of stretching.

The orignal mass of the string was 0.0135 ± 0.0005 kg. The total unstretched length of the string used for the experiment was 1.955 ± 0.0005 m. **Table 6.1** shows the data recorded for three different masses hung from the string.

Mass (kg)	String Length (m)	Tension (N)	Linear Mass Density μ (kg/m)	Wave Velocity (m/s)
0.202 ± 0.0005	1.979 ± 0.0005	1.983 ± 0.005	0.0069 ± 0.0002	17.0 ± 0.5
0.303 ± 0.0005	2.002 ± 0.0005	2.965 ± 0.005	0.0068 ± 0.0002	20.88 ± 0.07
0.403 ± 0.0005	2.034 ± 0.0005	3.946 ± 0.005	0.0067 ± 0.0002	24.3 ± 0.2

Table 6.1 Measurements recorded to find μ and wave velocity of the standing wave.

As more mass is hung from the pulley and more tension is applied to the string, the linear mass density decreases and the velocity increases.

Wave velocity can also be calculated by graphing the Light Intensity (%) and time (s) **Figure 6.7**. The wave velocity is calculated by dividing twice the length of the string between the pulley and clamp (distance a wave travels) and dividing it by the difference in time peaks. The distance a wave travels is 3.18 ± 0.005 m.

Mass (kg)	Time Interval (s)	Wave Velocity (m/s)
0.202 ± 0.0005	0.187 ± 0.005	17.0 ± 0.5
0.303 ± 0.0005	0.153 ± 0.005	20.8 ± 0.7
0.403 ± 0.0005	0.132 ± 0.005	24.1 ± 0.9

Table 6.2 Wave velocities measured by photodiode using time intervals of **Figure 6.8 (a), (b), (c)**.

The velocities calculated in **Table 6.1** and **Table 6.2** show that the velocities calculated from tension and μ and measured by the photodiode were within the same uncertainty range, and so our measured wave velocities are precise.

For the remaining parts of the experiment, the 0.4 kg weight was used to provide tension.

A vibrating spring will produce the greatest oscillations at the fundamental frequency, where there is one big wave traversing the string and 2 nodes of no movement on either end of the string. The wave produced is called an anti-node. Higher frequencies that are a multiple of the fundamental

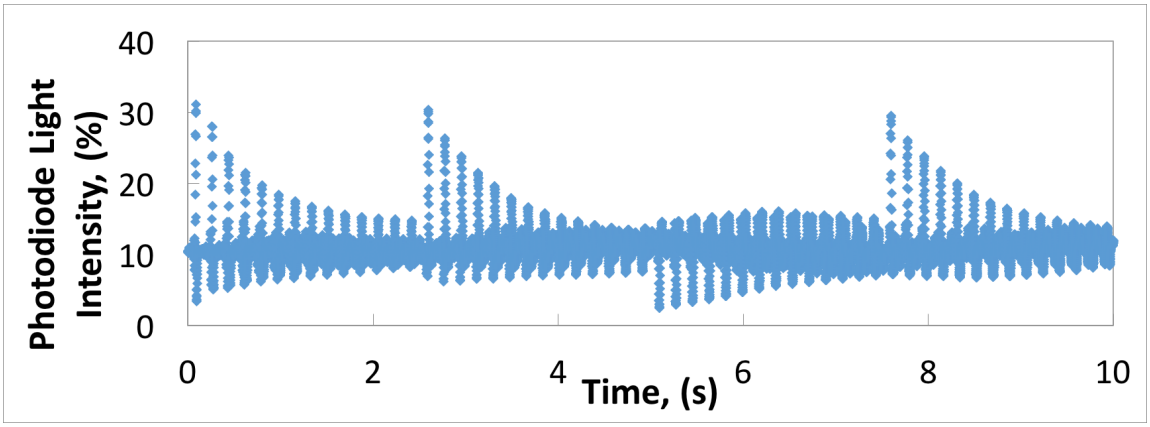

(a) Weight: 0.2 kg

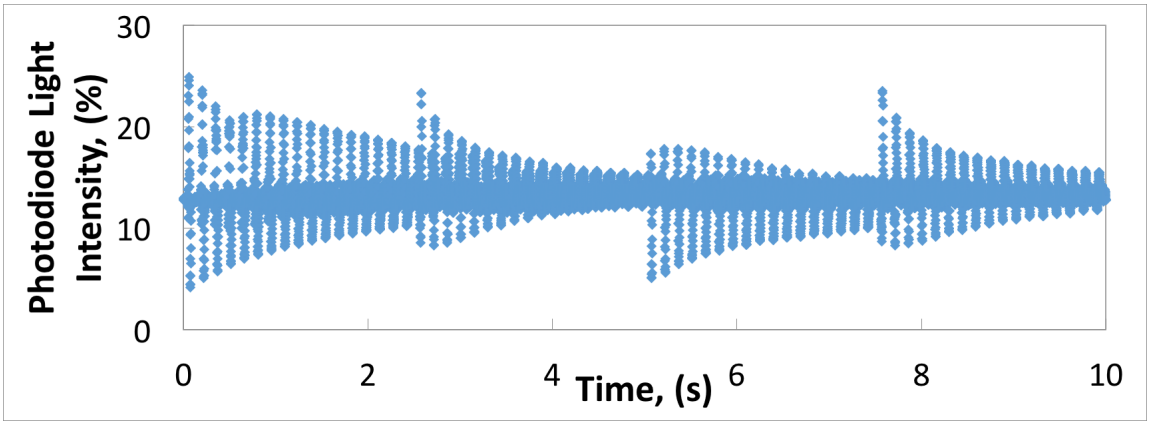

(b) Weight: 0.3 kg

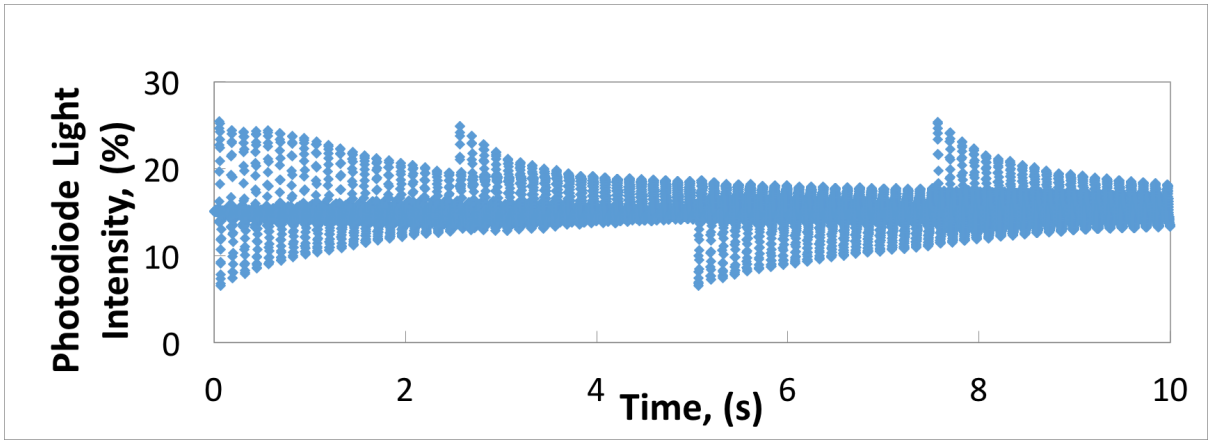

(c) Weight: 0.4 kg

Figure 6.8 Parametric plots of Angle (rad) vs Output voltage (V). (a) shows drive frequency below resonance, (b) shows drive frequency above resonance, and (c) shows drive frequency at resonance.

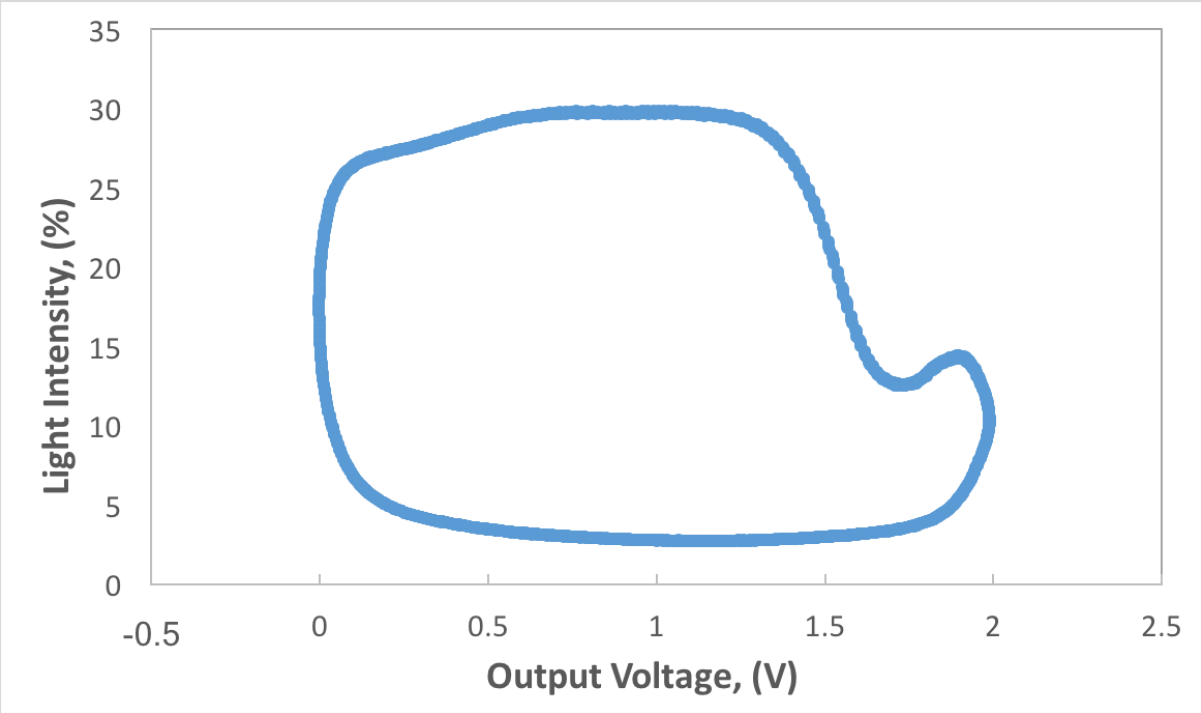

Figure 6.9 Light Intensity vs Voltage of Drive Frequency. The parametric plot was recorded at a drive frequency of 7.92 Hz.

frequencies produce more nodes and anti-nodes. We will try to find the frequencies that produces these nodes in the following analysis.

To identify the fundamental frequency, we used a Lissajous plot to tune the drive frequency until we found the Lissajous plot was as symmetric as could be. This plot is displayed in **Figure 6.9**. The fundamental frequency was found to be 7.92 ± 0.01 Hz.

Now that we have the fundamental frequency, the nth normal nodes should be close to or is a multiple of the fundamental frequency. The expression of the frequency of the nth normal mode is

$$f(n) = \frac{nv}{2L}$$

where n is the number of anti-nodes, v is the wave speed, and L is the length of the string. Using the velocity measured prior for the 0.4 kg weight and the length of the string, we approximated what the frequency should be and plotted Lissajous plots until we found a frequency that made the plot as symmetric as it could be. **Table 6.3** compares the calculated to measured values of the nth mode frequency.

Harmonic Number (n)	Measured Frequency (Hz)	Calculated Frequency (Hz)
1	7.92 ± 0.01	7.92 ± 0.01
3	23.81 ± 0.01	23.76 ± 0.04
5	40.02 ± 0.01	39.60 ± 0.07
7	55.78 ± 0.01	55.44 ± 0.09
9	71.44 ± 0.01	71.3 ± 0.1

Table 6.3 Measured and Calculated Harmonic Frequencies.

The measured frequencies were slightly higher than the predicted calculated frequencies, yet all the measured values were within the uncertainty values of the caluclated values, so our measurements are precise.

When a string is vibrating at a normal mode, there is no displacement at each node. Thus, if an object was placed on a node, it will should not interfere with the oscillation of the standing waves. We tested this by placing a clamp on in the middle of the string and vibrating the string at the frequencies that corresponded to $n = 2, 4$, and 5, and compared the amplitudes with and without the clamp. **Table 6.4** shows these amplitudes.

Harmonic Number (n)	Drive Frequency (Hz)	Signal Amplitude Unbounded	Signal Amplitude Bounded
2	15.84 ± 0.01	26.85 ± 0.01	26.7 ± 0.1
4	31.68 ± 0.01	23.14 ± 0.01	22.9 ± 0.1
5	40.02 ± 0.01	23.32 ± 0.01	0.3 ± 0.1

Table 6.4 Drive Frequency Ampltidues for bounded and unbounded string vibrations.

For the frequencies at $n = 2$ and $n = 4$, when bounded the amplitudes of oscillation decreased, but were still within the bounds of uncertainty. This is to be expected, as placing a boundary condition on a node should not affect the standing waves. However, at $n = 5$, there is almost no oscillation amplitude, because the boundary condition is placed right on top of a node, which almost cancels out the oscillations.

As an aside, we decided to see what the greatest mode of standing waves we could find. The theoretical max number of nodes that could be present on our stretched string would be 80 nodes, which found by taking the length of string from the pulley to the sensor, which was 0.02 m, and dividing that by the length of the total horizontal string. At n = 80, there will be a node directly underneath the photodiode laser, which will make it impossible to measure oscillations of a standing wave, because a node has no displacement. The greatest node we could find in our experiment was n = 20 however. Beyond n = 20, the standing waves became too small to detect.

CONCLUSION

The objective of this experiment was to study harmonic motion in two forms, the oscillations of a physical pendulum and the waves of a vibrating string. We first investigated the three regimes of damping, and found that when the magnets were spaced 15 ± 0.5 mm apart, we achieved critical damping, which is the point where the pendulum comes to rest at the equilibrium state fastest.

Using the same physical pendulum, we studied driven oscillations to measure the driving resonant frequency, which was determined to be 0.714 ± 0.005 Hz. At this frequency, we determined the Q-factor a driven oscillation at this frequency in two ways; first by measuring the amplitude values of various frequencies at and close to the driving frequency, and also by plotting Lissajous Figures and measuring the amplitude of the plots. The two values of Q obtained through these methods were completely outside their respective uncertainty boundaries, which we can attribute to systematic uncertainty due to the wave driver (when creating Lissajous Figures at the same frequency, the amplitude would differ between trials, thus causing systematic uncertainty in the experiment). Thus the first method of finding the Q-factor by taking measurements of many amplitudes at many frequencies is most accurate, because it helps eliminate systematic uncertainty, and so is more precise. The Q-factor was determined to be 3.76 ± 0.06.

For waves on a vibrating string, we found the wave speed caused by hanging three different masses (0.202 ± 0.0005 kg, 0.303 ± 0.0005 kg, and 0.403 ± 0.0005 kg) from the end of the string. The measured velocities were 17.0 ± 0.5 m/s, 20.8 ± 0.7 m/s, and 24.1 ± 0.9 m/s. All of the measured velocities are within the calculated velocity's uncertainty range, which indicates our measured velocities are precise.

With the same vibrating string, we also found the fundamental frequency by tuning the drive frequency until we produced a Lissajous Figure that was symmetric, which turned out to be 7.92 ± .01 Hz. Having found these values, we found the harmonic frequencies for modes n = 3, 5, 7, and 9. The measured frequencies were within the uncertainty range of the calculated frequencies (which should be the nth multiple of the fundamental frequency).

We also investigated boundary conditions of standing waves, at wave numbers of n = 2, 4, and 5. At n =2 and 4 we noticed that the amplitude of string oscillations decreased slightly with a constraint but still maintained a sinusoidal motion. This is because the boundary condition was placed right at a node in the standing waves, of which there should be no displacement already anyway. In contrast, at n =5 the boundary condition was placed right on top of an oscillating wave, and so the constraint cancelled out the wave and reduced the oscillation amplitude to almost zero. Because the constraints we used were blocked more than a single finite point on the string, a small part of the oscillating string was caught by the constraint for trials at n =2 and 4, which explains the slightly lower oscillation amplitudes compared to their unbounded oscillations.

REFERENCES

1. Campbell, W. C. et al. Physics 4AL: Mechanics Lab Manual (ver. April 3, 2017). (Univ. California Los Angeles, Los Angeles, California).